BNL-tr--1015

DE84 004551

RESULTS OF THE EXAMINATION OF CHANNEL H12/1

By E. Bauer

Translated from the French* Report RHF No. 106 dated Jan. 20, 1983
EB/GG/83/106

*Translated by LANGUAGE SERVICES, Nashville and Knoxville, TN

RESULTS OF THE EXAMINATION OF CHANNEL H12/1

TABLE OF CONTENTS

1. INTRODUCTION

Channel H12/1 is part of the channel unit of the High-FLux Reactor (HFR) characterized by the designation: average corrosion attack. It was disassembled after the appearance of a heavy water leak.

The front part of the channel was preconditioned in the hot cell of the HFR and sent to the Karlsruhe KERNFORSCHUNGSENTRUM (KFK - Germany) where all the work required by the research was performed.

2. DESCRIPTION OF CHANNEL H12/1

Channel H12/1, which is made of AG 3 NET aluminum alloy is placed horizontally in the reflecting can, 250 mm below the median plane of the core.

Its axis is oriented tangentially with respect to a 450 mm radius circle whose center is the axis of the reflecting can.

However, the distance between the front end of the channel and the tangent point is approximately 400 mm.

The total length of the channel is approx. 4.8 meters with a length of approximately 1.4 m of the forward overhanging portion.

Figure 1 gives the details of the configuration of the end of the channel.

The nose "a" is composed of a hemisphere (thickness 2 mm, interior diameter 100 mm) and of a conical end (length 30 m, thickness 4 mm) done by stamping. The nose is connected to a conical ferrule "b" (thickness 4 mm) by a circumferential weld.

The conical ferrule, made from a rolled sheet, has a longitudinal weld. At the time of the manufacture, the weld beads of the front portion were leveled. The exterior surface has undergone a passivation treatment.

The channel is submerged in the heavy water of the reflecting can and its interior is filled with helium. The pH of the heavy water is between 5 and 5.5.

While the reactor is operating, the temperature of the front end of the channel can be estimated at approximately 70°C, and the temperature of the rear portions at approximately 50°C.

Channel H12/1, which has been in place since the beginning, was disassembled on 7/22/82, which corresponds to irradiation for 2,395 days

equivalent at full reactor power. The dose of thermal neutrons received by the front end can be estimated at 1.7 . $10^{23} n_{th}/cm^2$.

The portion of the channel to be used in the research was conditioned in the hot cell of the HFR so that a length of approximately 1.2 m from the front end could be sent to KFK [Karlsruhe].

3. OBSERVATIONS

As previously with channel H13/1, two series of photos were taken in the hot cell:

--a first series related to the appearance of the channel with its deposit of alumina;

--a second series after washing of the channel with demineralized water.

The two series of photos were taken so that all of the channel surface would be shows on the corresponding photos.

3.1. Raw channel

Figures 2 to 7 whos the appearance of the channel prior to washing. The channel is covered with a deposit that is thicker on the front end side (figures 2 and 7) than on the back side (figures 2 and 5).

In the intermediate portions (figures 3 and 6) considerable traces of handling are visible. The deposit is thinner than in the front portion.

The two series of photos (2 to 4 and 5 to 7) relate to the side of the channel that was in a direct line of the fuel element. Even under the deposit layer, white dots whose number is greater on the side of the hemispherical bottom can be seen clearly.

The weld bead connecting the hemispherical bottom to the conical ferrule is scarcely visible (figure 4 and 7).

3.2. Washed channel

The appearance of the channel after washing is given on figures 8 to 13 so that each photo relates to a sector that was shown on photos 2 to 7.

The weld beads appear clearly. Specifically, we see a triple weld bead (figures 10 and 13) in the juncture between the hemispherical bottom and the conical ferrule.

With the exception of the white dots, the channel has a clear and regular appearance. The white dots are concentrated in the front portion. The last white dot is visible approximately 25 cm from the hemispherical nose. A superficial examination does not allow us to reveal the zone that caused the leak [lack of water tightenss] observed.

The weld bead connecting the hemispherical bottom to the conical ferrule shows traces of corrosion between two visible weld beads (fig. 14).

These traces of corrosion resemble the traces observed on the conical ferrule to the right and on the hemispherical bottom, to the left of the weld bead (fig. 14).

An attempt to blow up the channel with compressed air and the application of soapy water to the exterior made it possible to reveal the zone where the leak took place. In fig. 15 it is located in the hemispherical nose, slightly above the axis of the channel.

In fig. 16 it is located at the very top of the channel.

The front end of the channel was treated with methyl alcohol so as

to emphasize the contrast between the defective zone and the nearby material (fig. 17). It is a long defect, in the shape of an inverted L. On the end is placed a circular zone. In the point of the L there is an extended zone that appears dark. The opposite end is also formed by a circular zone located in the portion of the nose that is 4 mm thick. In the basically vertical portion there is an extensive zone that also appears dark. The total length of the elongated defect can be estimated at approximately 7 cm.

Figure 18 shows details of the defect. To the left of the figure there is the beginning of the defect of a circular shape. In the central portion of the figure are two extensive zones appearing dark on figure 17.

A shadow effect can be clearly distinguished in the extensive upper portion, indicating that it is a recessed surface compared to the channel surface.

Figure 19 shows the interior appearance of the channel opposite the zone that caused the leak. We see two traces of flow. At the bottom of the figure corresponding to the lower portion of the channel a dark zone can be seen. The traces delimiting this dark zone suggest that it is a coloration caused by the presence of leaking water in the channel. There is also a considerable collapse of the circular weld bead.

3.3. Sweating out test

A sweating out test was done in cell to reveal the presence of possible cracks.

The method used corresponds to the process usually applied:

--application of a penetrant followed by application of a revealing agent that undergoes a change of color opposite the crack.

The zones involved by the test are located in approximately 15 cm in

the front of the channel. In addition, two strips 8 cm wide located on the upper and lower generatrices were subjected to the test.

At the end of the test, the white dots visible on the photos took on a red coloration. No additional defect, outside the defective zone, was observed.

4. METALLOGRAPHS

Figure 20 shows the location of the specimens that were used for the metallographs.

No. 1 defective zone: see figure 17
No. 2 white dot in the hemispherical portion: see figure 16.
No. 3. White dot in the hemispherical portion: see figure 16
No. 5 white dots in the weld bead: see figure 14
No. 6 white dot in the conical ferrule: see figure 13.

The figure numbers indicates the photos that give the appearance of the specimens on the washed channel. The white dots are found in the intersection of the horizontal and vertical lines designated by the specimen number.

4.1. Defective zone (specimen 1)

4.1.1. Description

Figure 21 gives the schematic representation of the defective zone with indication of the metallograph planes.

The defect is composed of a circular zone A, of an elongated defect that connects defect A to a white dot C and of a burst zone E connected to the white dot by an elongated defect D.

The metallographs were made along planes parallel to each other, indicated schematically in figure 21.

Table I gives the definition of the metallograph planes with the distance Δ between two neighboring planes and the distances between a given plane and plane A, $\Sigma\Delta$.

Figures 22 to 25 show the metallographs related to the circular zone A. It can be seen that the circular zone visible on figure 17 is constituted by a burst zone 0.5 mm thick maximum. The diameter can be estimated at approximately 6 mm. Below this zone separated from the base material there are two cracks oriented diagonally to the direction of the circumference.

These are essentially straight cracks, very fine, in plane "a", thicker in plane "d". The angle included between the direction of the crack propagation and the circumferential direction varies by approximately 10° (plane "a") to 15° (plane "d"). The principal crack visible in plane "d" opens to the exterior side (D_2O) and is non-opening to the interior.

Small cracks appear in the large crack separating the base material and the completely separated zone.

The elongated defect B, visible on figure 17, is constituted by the opening portion of the principal crack in plane "d" that takes on magnitude (figure 26) and becomes opening, also to the interior, the helium side (figure 27).

The angle between the direction of progress of this crack and the circumference direction increases to 20° (figure 26) and to 24° (figure 27). The width of the crack in plane "f" is approximately 0.1 mm. In the zone with the white dot (figure 28 and 29) the principal crack has a tendency to separate into several branches, still limited in plane "g", in a more pronounced fashion in plane "h", where two preferential orientations of propagation of the crack can be observed:

--26° for the principal crack
--approximately 9° for the cracks separating from the principal crack.

DEFINITION OF THE METALLOGRAPH PLANES

PLANE REFERENCE	Δ	ΣΔ	ZONE REPRESENTED	FIGURE
a	--	--	A: circular zone	22
b	0.5	0.5	A: " "	23
c	0.4	0.9	A: " "	24
d	2.4	3.3	A: " "	25
e	1.2	4.5	B: elongated defect	26
f	1.3	5.8	B: elongated defect	27
g	3.0	8.8	C: white dot	28
h	6.3	15.1	C: white dot	29
i	2.2	17.3	D: elongated defect	30
j	4.2	21.5	E: burst zone	31
k	0.2	21.7	E: burst zone	32
l	0.2	21 9	E: burst zone	33

Δ : Distance between two neighboring planes

ΣΔ : Distance between a plane and plane a

The depth of attack in the zone with the white dot (figure 29) is about 0.7mm. Small cracks oriented in the circumferential direction that start in the principal crack can also be observed. It can be assumed that the bottom of the white dot has been constituted from a crack oriented in the circumferential direction.

The elongated defect D is given by the opening portion of the principal crack. The other cracks have a tendency to disappear gradually.

Figures 31 to 33 show the metallographs in the burst zone E. The principal crack is oriented at 28° to the circumferential direction (plane j) at 25° (plane 1). The shape of the bottom of the burst zone suggests that the bursting was due to the joining of a crack oriented essentially in the circumferential direction with the principal crack.

The maximal depth of the burst zone reaches 0.9 mm (plane j), its width approximately 5mm.

The walls located on either side of the crack are off-set by approximately 0.1 mm. The width of the principal crack reaches approximately 0.2 mm (plane 1).

The observations can be summarized as follows:

-- the water tightness defect is due to the presence of a crack opening to the exterior and to the interior, oriented from 15° to 30° approximately to the circumferential orientation of the nose represented on the metallographs.

-- in places, other cracks form, oriented differently, that constitute the white dot or the burst zone, depending on the preferential direction of their progress.

-- The depth of these other zones reaches approximately 0.9mm (zone E) and 0.7 mm (zone C).

-- The material located on either side of the principal crack was displaced by approximately 0.1mm.

4.1.2. Details of the cracks

Figure 34 shows the differences between fine cracks and broad cracks, such as those that separate the detached portion of the base material in plane "a".

The metallograph was treated so as to reveal the grain boundaries of the material as well as the shape of the grains.

The small crack follows the grain boundaries perfectly, which means that its shape is not regular. The two edges of the crack have an identical shape. The crack has a tendency to detach the grains from each other (figure 35).

The large crack separating the detached portion of the base material has rounded edges, much more regular than the small crack. The same remarks are also valid for tthe metallographs of the other planes. Figures 36 and 37 show details of the cracks that are close to the interior edge.

The small crack at the top of photo 36, as previously, has a shape that prefectly retraces the grain boundaries. Its edges have identical shapes.

The principal crack has edges that are rather rounded and the two edges do not have an identical shape.

Figure 38 showing the principal crack in plane "g" hardly allows the shape of the grains the limit the crack to be recognized.

The principal figure of plane "h" (figure 39) gives rise to the same remarks. In addition, we see the formation of small caves on the edges of the principal crack. In places, these caves become small cracks

that have the same appearance as the small cracks previously presented.

The metallographs given in figures 34 to 37 were prepared so as to reveal the grain boundaries. In all of the cases shown, the grains have an elongated and irregular shape, showing a preferential orientation.

This preferential orientation corresponds to the direction of propagation of the small cracks (figures 35 and 37).

Figure 40 shows a detail of the cracks in plane "e" in normal light. The same portion is shown in figure 41, taken in polarized light.

The cracks with a normal appearance (figure 40) show, under polarized light, a clean structure that indicates that the crack is filled with material.

The structure gives the crack the appearance of being filled with plugs delimited by perpendicular planes in relation to the edges of the crack. Given that, in figure 41, the two ends of the cracks are involved, this material that fills the crack must be constituted by corrosion products.

4.1.3. Crack formation

The analysis of the appearance of the cracks and of their edges makes it possible to describe the processes of formation of the cracks that are visible on the various metallographs.

The first cracks, very fine, are formed in the direction of orientation of the grains. These cracks become increasingly thick, thus pushing back the material separated by the crack.

During a second period, the edges of the crack are attacked so the irregular shape of the edges to the shape of the grains delimiting them disappears. Gradually smooth walls form with a tendency to reveal a caving attack similar to that observed on the exterior surface of the channel (figures 22 to 33).

To the extent that the number of small cracks increases, portions of the material are found completely detached, giving rise to a relatively great attack surface. The attack of more or less detached grains causes a certain quantity of the material to disappear and brings about the freeing of large portions of the material.

Given the preferential orientation of the grains in the portion examined, the propagation direction of the principal crack was oriented from the exterior towards the interior, which provoked the loss of tightness of the channel.

4.2. WHITE DOTS ON THE HEMISPHERICAL BOTTOM

The two largest dots on the hemispherical bottom are shown in figures 42 and 43.

In both cases, it is a laminating corrosion attack. However, the cracks are limited in number and there are elements of caving attack in both cases. The depth of attack is 0.25 mm (specimen 2) and 0.45 mm (specimen 3). In both cases, a development of fine cracks towards the interior of the material cannot be noted.

4.3. WELD BEAD CONNECTING THE CONICAL FERRULE TO THE HEMISPHERICAL BOTTOM

Figure 44 shows an overall view of the weld bead opposite a white dot visible on figure 14.

The preparation of the metallograph causes the heat-affected zones to be visible in the form of slightly darkened lines.

The final weld, which appears to be generally dark, is surrounded to the left by two weld beads:

--The base pass
--the filling pass

To the right another weld bead may also be seen. This indicates that the weld was repaired twice in a row. The corrosion attack took place in the zone that traces the boundary between the final weld bead and the bottom bead welded first of all.

The depth of the visible attack is approximately 0.5 mm. Figure 45 gives a detail of this corrosion zone. The appearance of this zone differs clearly from the appearance of the white dots or the cracks previously examined. It is rather a caving attack, with a smooth and rounded bottom. In no case can the formation of fine cracks starting from this cave be noted.

Figure 46 shows the same zone lighted by polarized light to reveal the orientation and the size of the grains. It is obvious that the bottom bead has been subjected to a considerable grain enlargement at the time the final weld was made.

For the sake of comparison, the size of the grains in the nearby material, except for the heat-affected zones, is visible on the same figure to the left. This considerable grain enlargement decreases the corrosion resistance of the weld bead and explains the formation of this corrosion pit.

4.4. CONICAL FERRULE

One of the white dots in the conical ferrule is shown in figure 47.

The attacked zone has a diameter of about 6 mm. Its depth is 0.4 mm.

The appearance of this attacked zone resembles the appearance of the white dots found on the hemispherical bottom (figures 42 and 43). The detail of this attacked zone shows the presence of small cracks starting at the principal crack (figure 48). However, the number of these cracks, as well as their size, is limited.

5. SILICON ANALYSIS

Figure 20 shows the location of the specimens for chemical analysis.

Specimen no. 10 is located about 1 meter from the end of the channel. Consequently, it is exposed to a relatively low flux.

Specimen no. 9 is located 250 mm from the front end. Its location corresponds to the appearance of the first traces of corrosion.

Specimens nos. 8 and 7 are in the zones that are clearly more irradiated.

Table II gives the measured silicon contents as well as the corresponding doses of thermal neutrons, calculated on the bases: 0.2 % silicon formed corresponds to a dose of $10^{22} n_{th}/cm^2$.

Table II

RESULTS OF SILICON ANALYSIS WITH CORRESPONDING DOSES

No.	Si content measured (% mass)	Increase (% mass)	Dose in thermal neutrons ($10^{22} n_{th}/cm^2$)
Ch A 10	0.18		
Ch A 9	1.74	1.56	7.8
Ch A 8	2.03	1.85	9.25
Ch A 7	(1.64)	(1.46)	(7.3)

The silicon content measured for specimen no. 10 corresponds to the content specified for AG 3 NET. Consequently, the dose received of the material at this point is very low and can be considered as negligible.

Specimen 9, representative for the material that begins to show traces of corrosion, has a content of 1.74% silicon.

If one considers the measured content for specimen 10 (0.18%) as the content of the non-irradiated material, the increase of the silicon

content corresponds to 1.56%, which represents a dose of thermal neutrons of $7.8 \cdot 10^{22} n_{th}/cm^2$.

The silicon content of specimen no. 8 is 2.03%, which corresponds to a dose of thermal neutrons of $9.25 \cdot 10^{22} n_{th}/cm^2$.

The measured value for specimen no. 7 (1.64% silicon) is too low to represent reality, considering the location of this specimen in the channel.

There was probably an error in measurement. The results will not be considered.

6. SUMMARY

Channel H12/1 which had a defective watertightness was examined in hot cell.

On the washed channel the leak location cannot be revealed by a superficial examination. The channel exhibits white dots on the forward portion. The zone involved included the 25 cm starting at the nose.

With the exception of these white dots, the surface of the channel has a regular appearance. It is light grey satin colored.

The leaking zone made visible by a treatment of reinforcement of contrasts has the shape of an inverted L. Its developed length is about 7 cm.

A sweating out test on the channel shows the absence of cracks or other anomalies beyong the zones involved by the white dots and by the zone that produced the defective tightness.

The defective zone is composed of a circular defect, of ellongated defects, of a white dot and of a burst zone.

The loss of water tightness is due to a principal crack that developed from the exterior towards the interior. Other small cracks starting in the principal crack produce a network of cracks around the principal crack.

All of the cracks are oriented in the direction of the preferential orientation of the ellongated grains of the material.

The white dots in the hemispherical bottom and the conical ferrule exhibit a caving attack with fine cracks oriented along the preferential orientation of the grains.

The depth of attack is between 0.25 mm and 0.4 mm.

The attack visible in the weld bead connecting the hemispherical bottom to the conical ferrule is due to a repair that caused considerable enlargement of the grains in the first weld bead. There is a caving attack without development of small cracks on the edges of the crater.

LIST OF FIGURES

22-25 Metallographs of the defective zone
Circular zone A 20:1

26-27 Metallographs of the defective zone
Ellongated defect B 20:1

28-29 Metallographs of the defective zone
White dot C 20:1

30 Metallograph of the defective zone
Ellongated defect D 20:1

31-33 Metallographs of the defective zone
Burst zone E 20:1

34 Detail of the crack and the detached portion (plane a)
100:1

35 Detail of the crack (plane a)
200:1

36 Detail of the cracks, inside side (plane h)
200:1

37 Detail of cracks, inside (plane h)
500:1

38 Detail of the principal crack (plane g)
200:1

39 Detail of the principal crack (plane h)
200:1

40 Detail of cracks (plane c)
Ordinary light 500:1

41 Detail of cracks (plane c)
Polarized light 500:1

42 Hemispherical bottom specimen No. 2
20:1

43 Hemispherical bottom specimen no. 3
20:1

44 Weld bead
General view 20:1

45 Weld bead, attacked zone
100:1

46 Weld bead- crystalline structure opposite pit 30:1

47 Conical ferrule specimen No. 6 20:1

48 Conical ferrule specimen no. 6 Detail 200:1

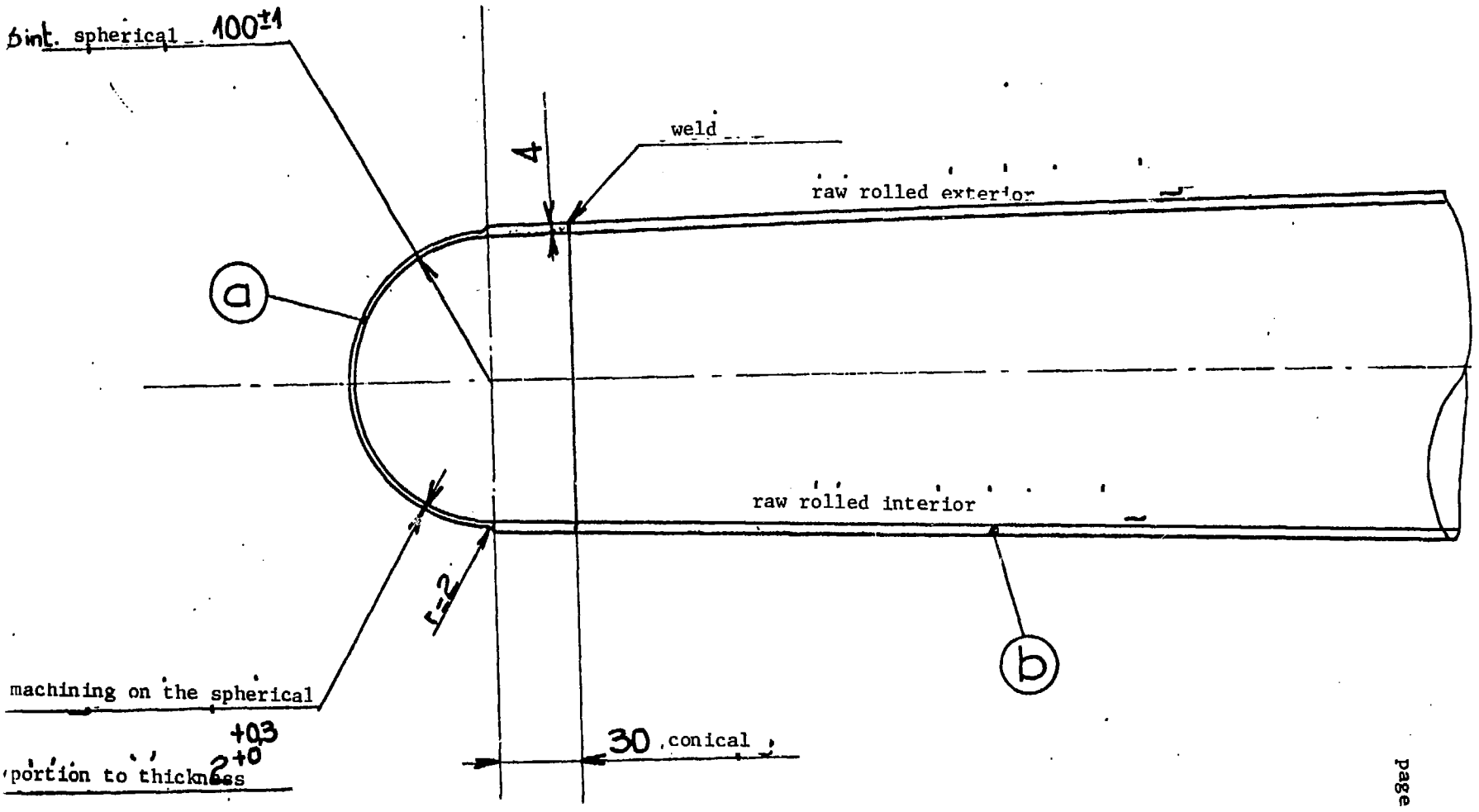

Figure 1 Channel H12/J Forward portion

AG3NET-RHF H12/1 Raw channel

2

3

AG3NET-RHF H12/1 Raw Channel

5

6

AG3NET-RHF H12/1 Washed channel

8

9

AG3NET - RHF H12/1 Washed Channel

11

12

1

6

1

6

1

6

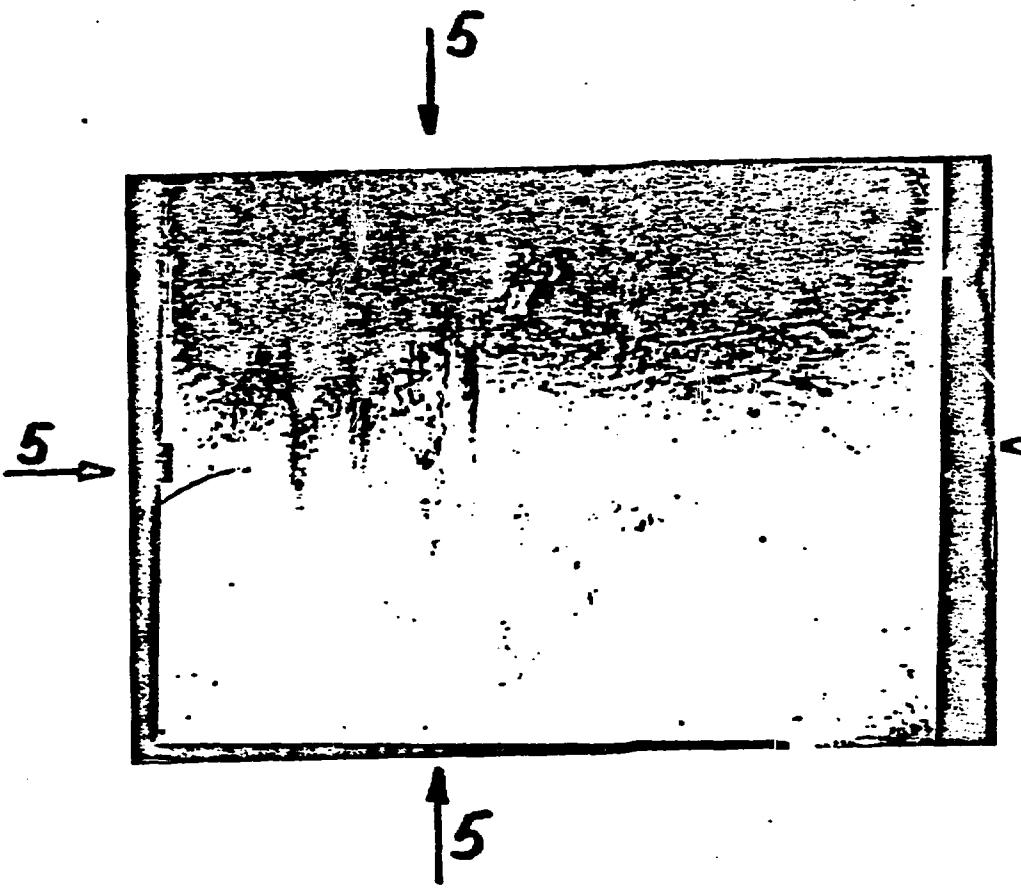

Fig. 14: Weld Bead

AG3NET - RHF H12/1 Washed Channel

15

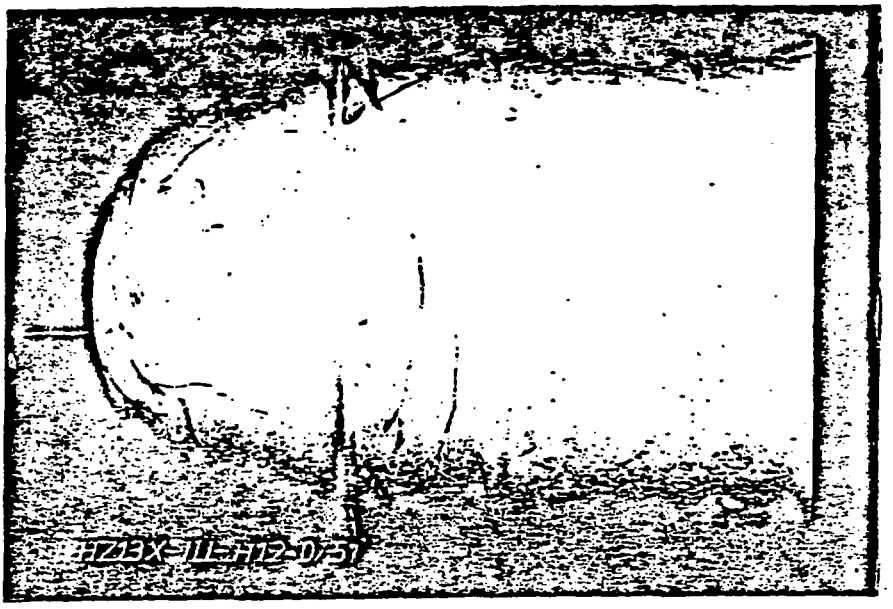

3 1 2

1 3 2

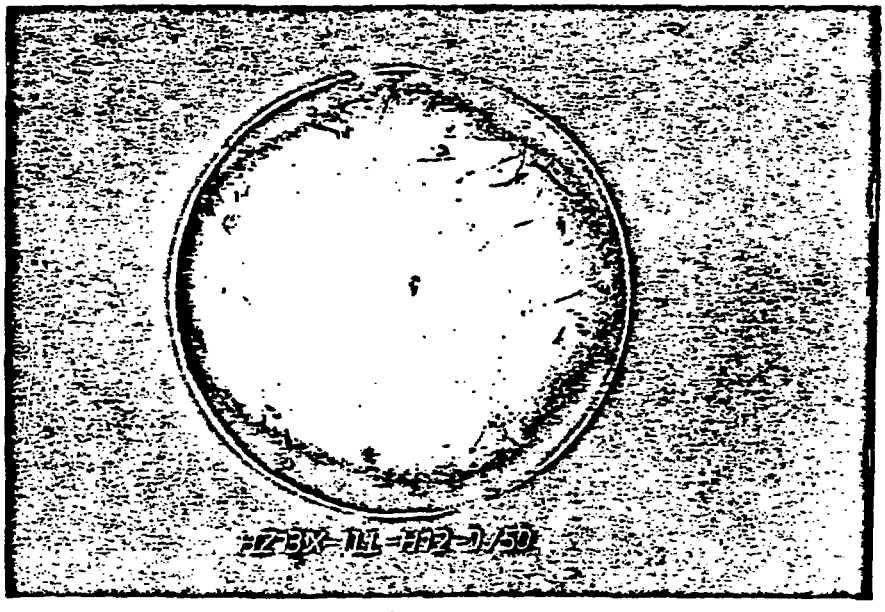

1 3 2

16

3 1 2

AG3NET - RHF H12/1 Defective zone

17

18

AG3NET-RHF H12/1 Defective zone

8 19

------ : Weld bead

○ : Water tightness defect

□ : Specimen with reference

Met... : Specimen number - Metallograph

ChA... Specimen number - chemical analysis

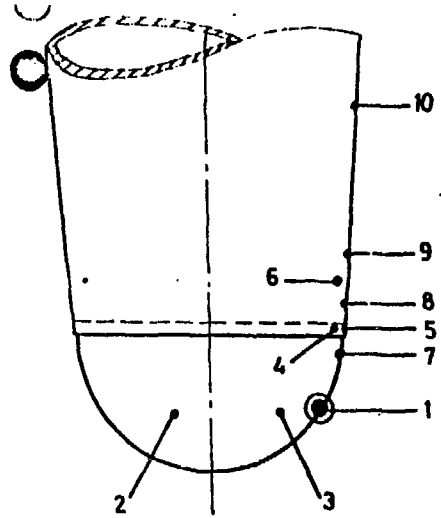

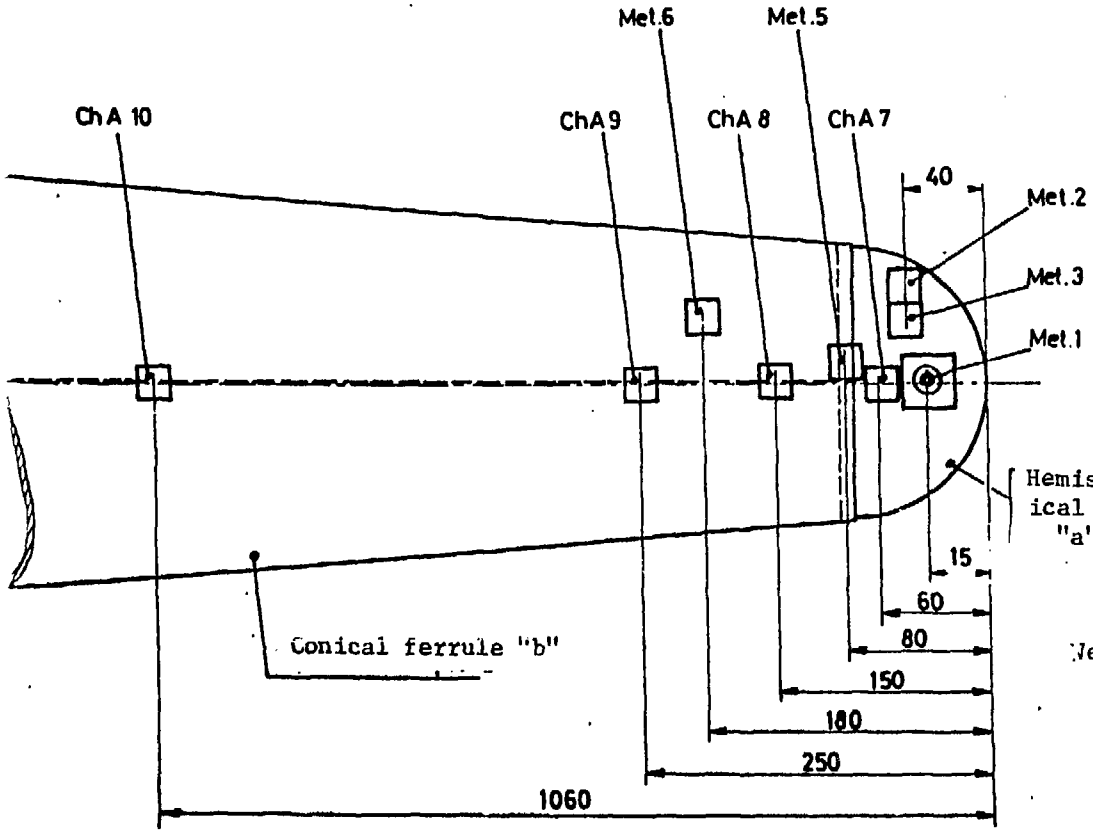

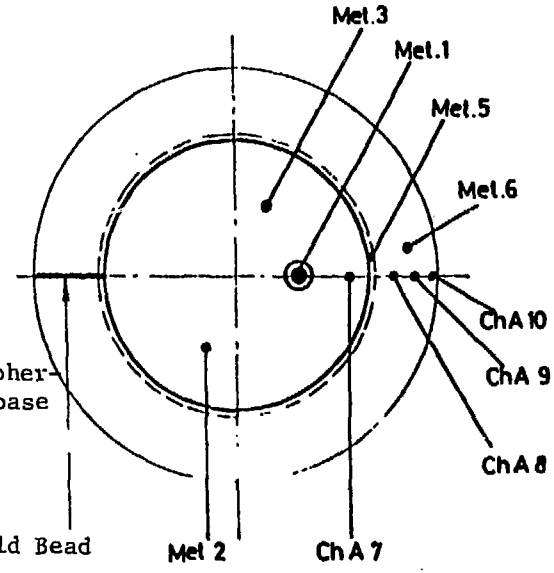

Fig: 20 LOCATION OF METALLOGRAPH AND CHEMICAL ANALYSIS SPECIMENS

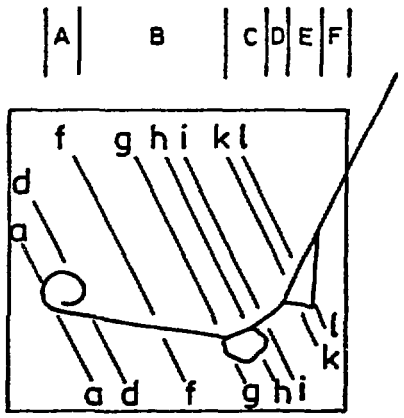

ZONE DESIGNATION

A : circular zone
B : Ellongated defect
C : White dot
D : Ellongated defect
E : Burst zone
F : Ellongated defect

Fig .21 – Schematic representation of the defect zone wiht indication of the metallograph planes (a-l)

10

AG3NET-RHF H12/1 Zone A plan

22

10 AG3NET-RHF H12/1 Zone A plan

23

AG3NET-RHF H12/1 Zone A plane C

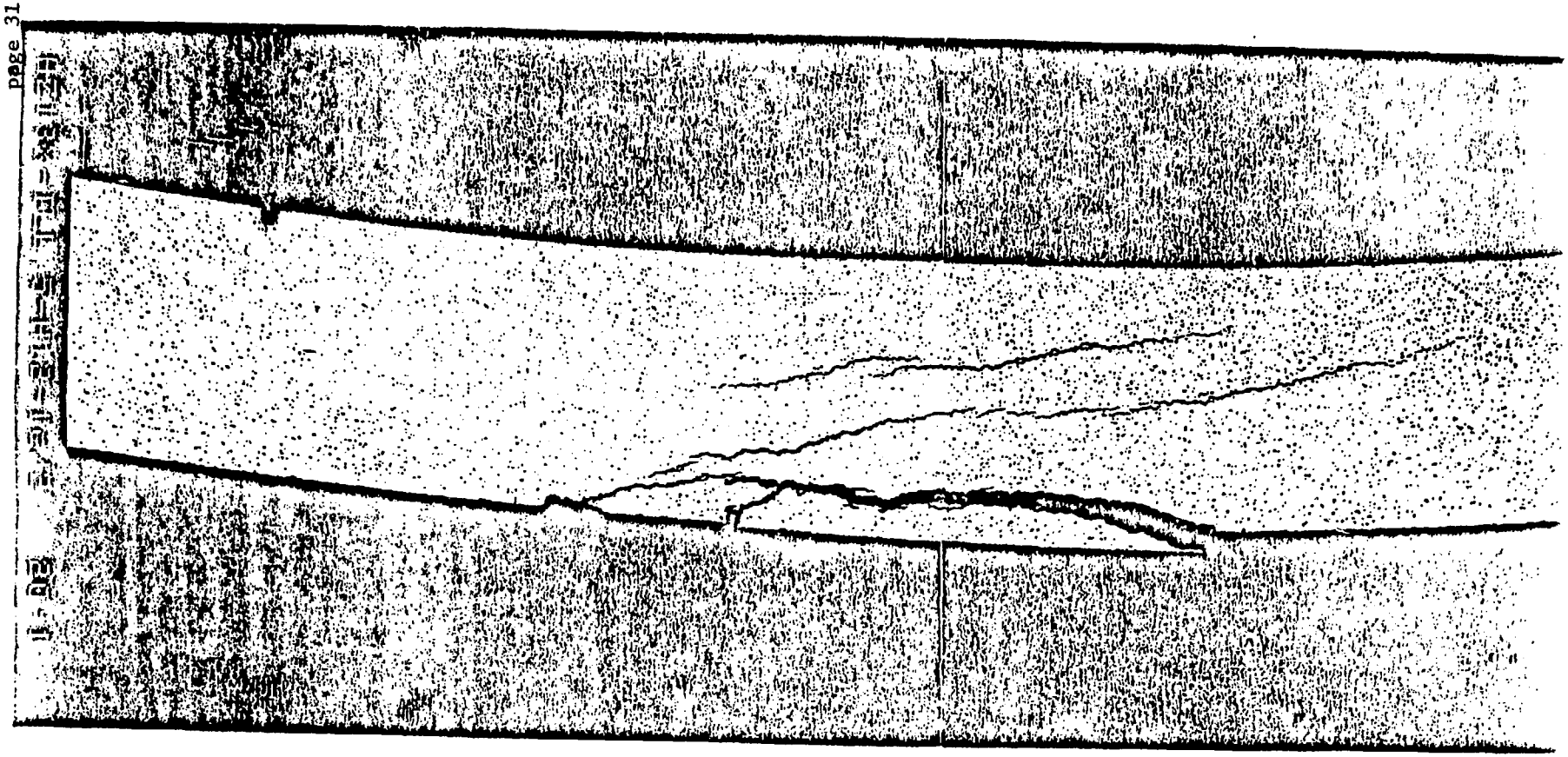

1d AG3NET-RHF H12/1 Zone A plan

12

AG3NET-RHF H12/1 Zone B plane

26

14

AG3NET-RHF H12/1 Zone B plan

27

19 AG3NET-RHF H12/1 Zone C plang

28

AG3NET-RHF H12/1 Zone C plan

29

12 AG3NET-RHF H12/1 Zone D plani

30

AG3NET-RHF H12/1 Zone E plane j

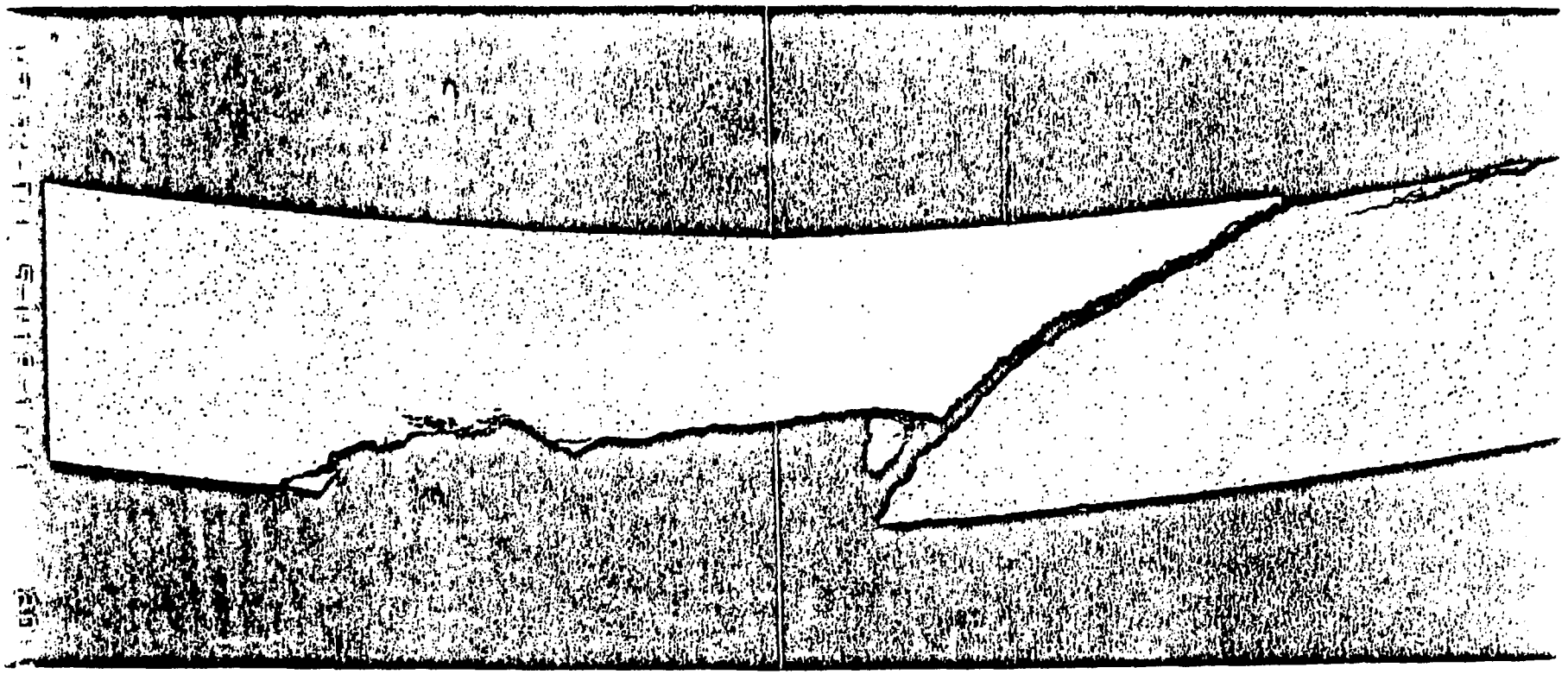

1k AG3NET-RHF H12/1 Zone E planek

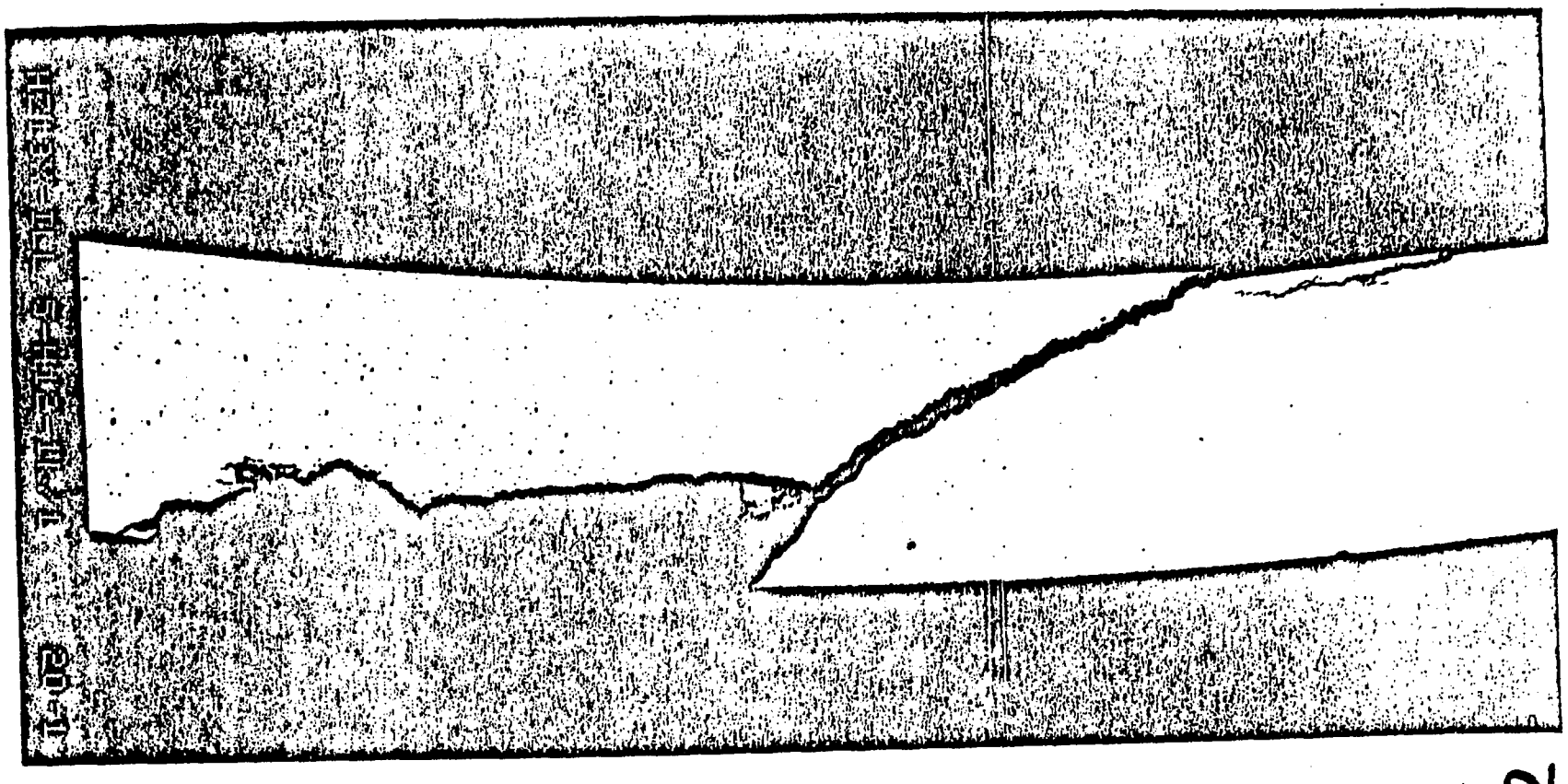

AG3NET-RHF H12/1 Zone E panel

33

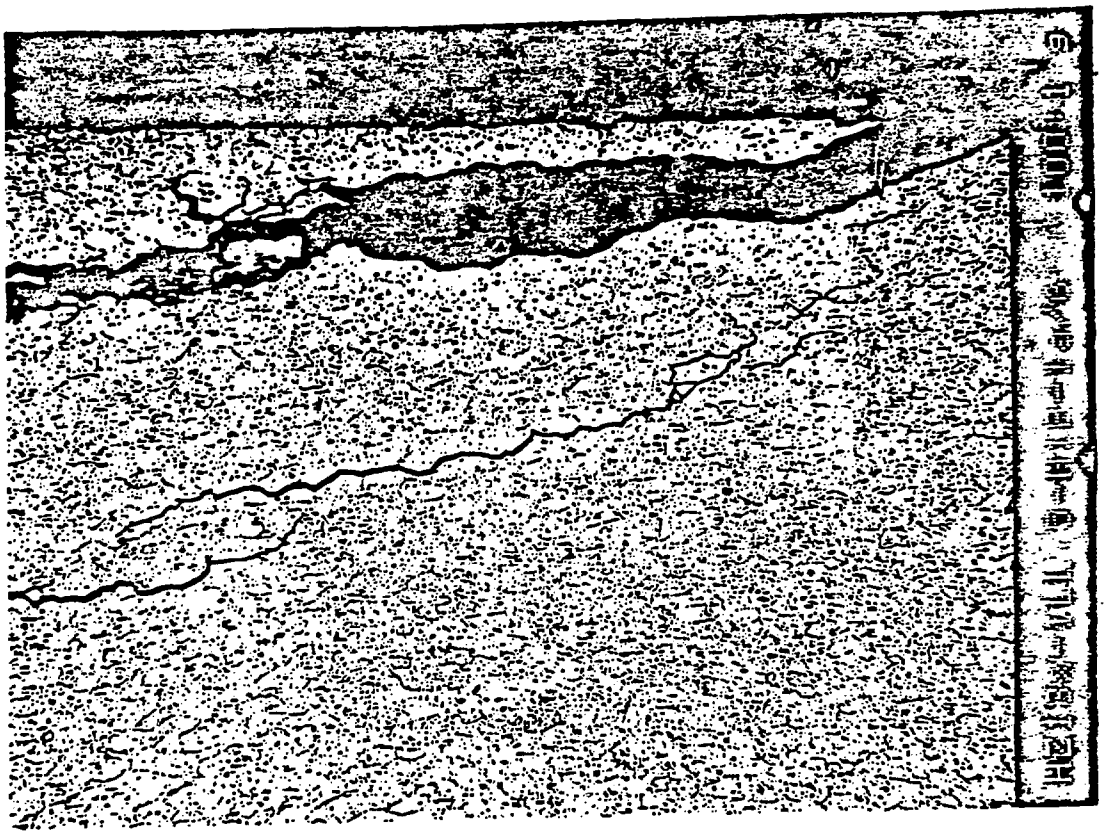

34 : Detail of crack and of detached portion (plane a)
100 : 1

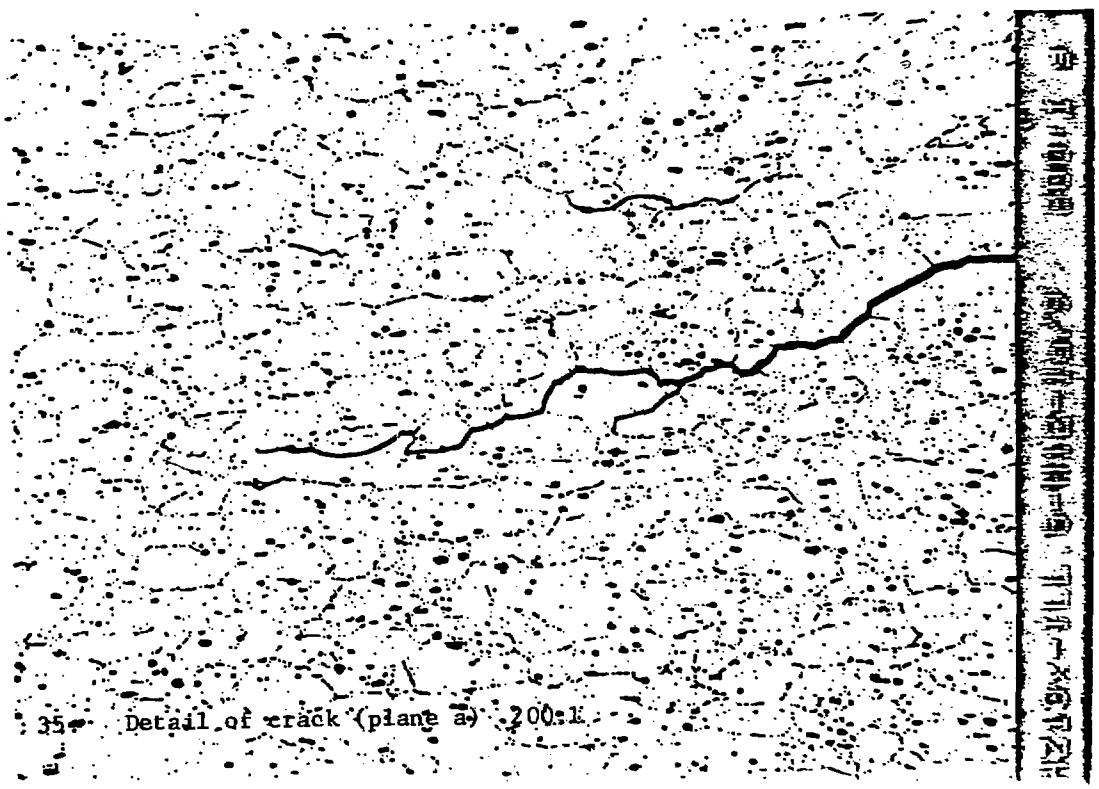

35 : Detail of crack (plane a) 200:1

36 : Detail of cracks, inside (plane n)

200 : 1

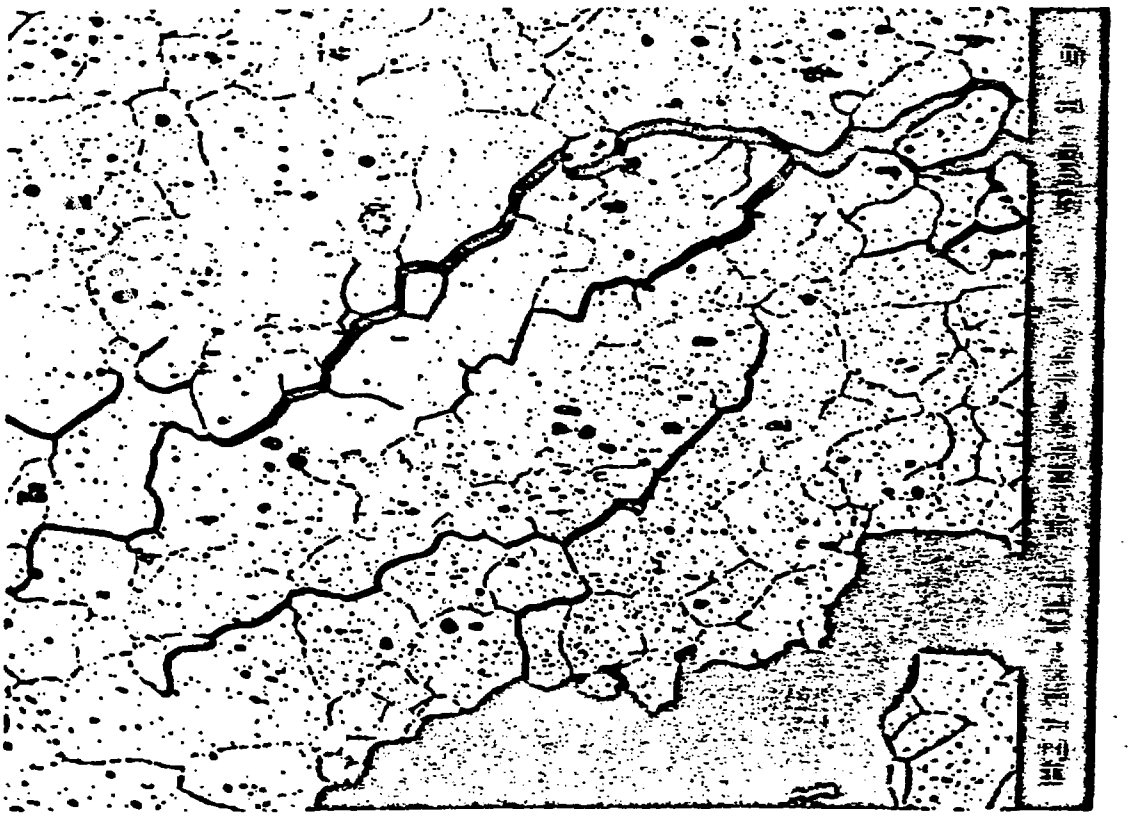

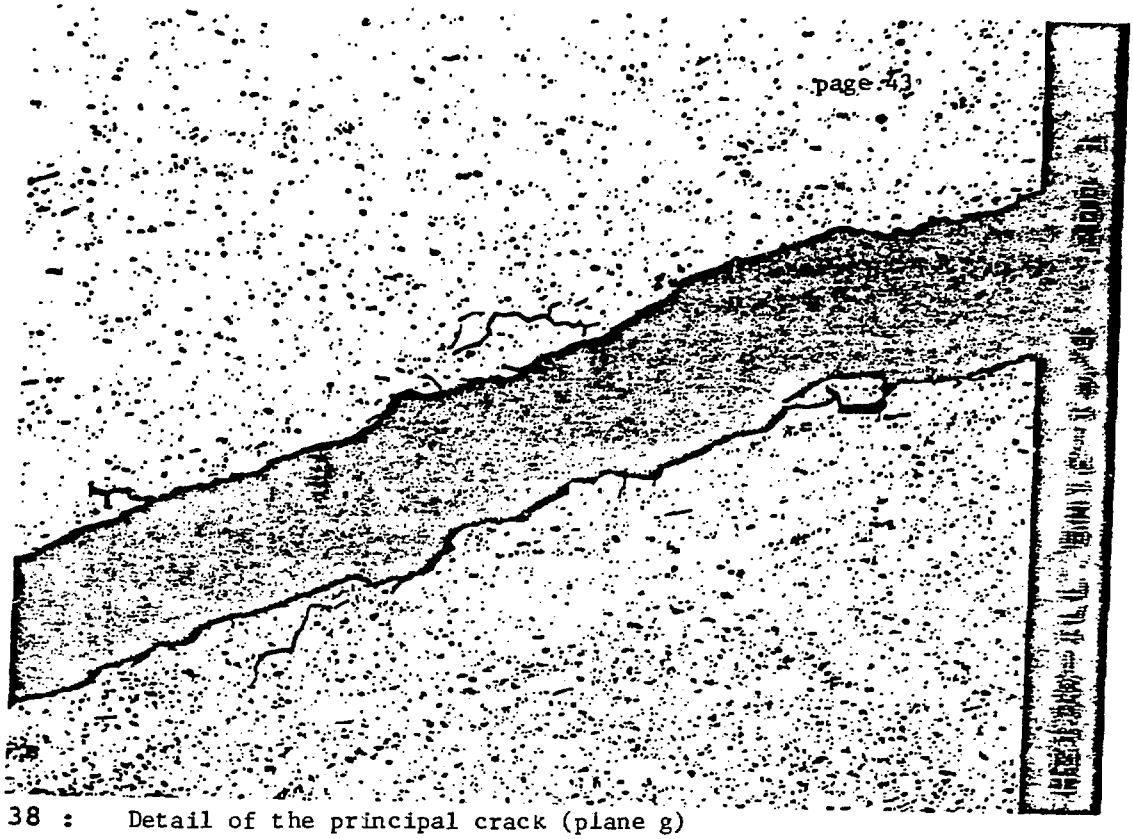

38 : Detail of the principal crack (plane g)

200 : 1

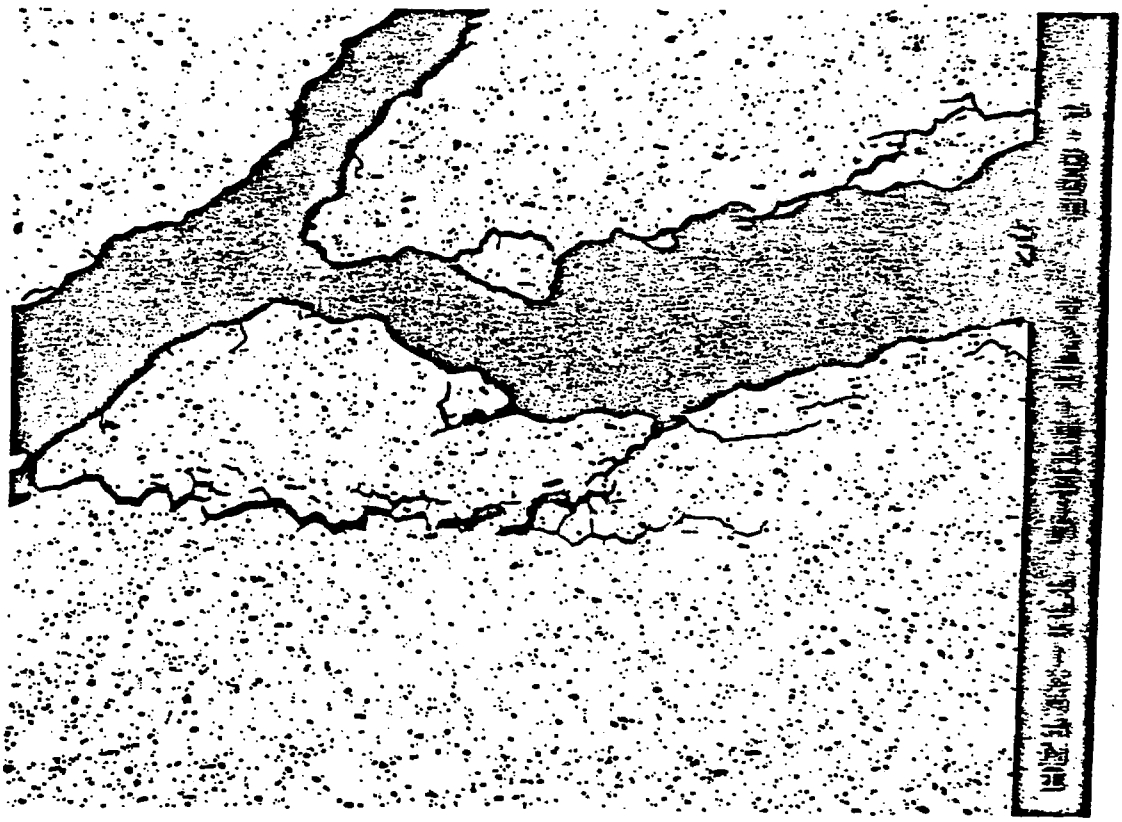

39 : Detail of the principal crack (plane h)

40 : Detail of cracks (plane c)
Ordinary light — · — · — 500 : 1

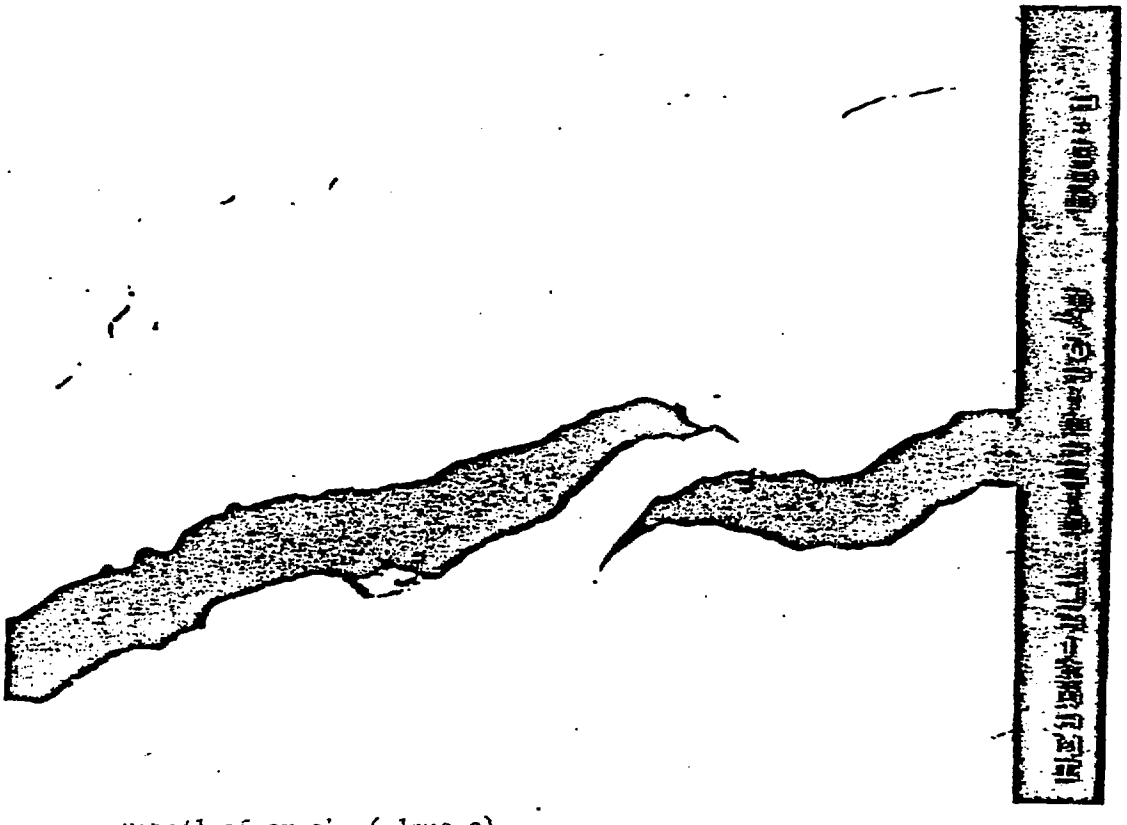

41 : Detail of cracks (plane c)
Polarized light 500 : 1

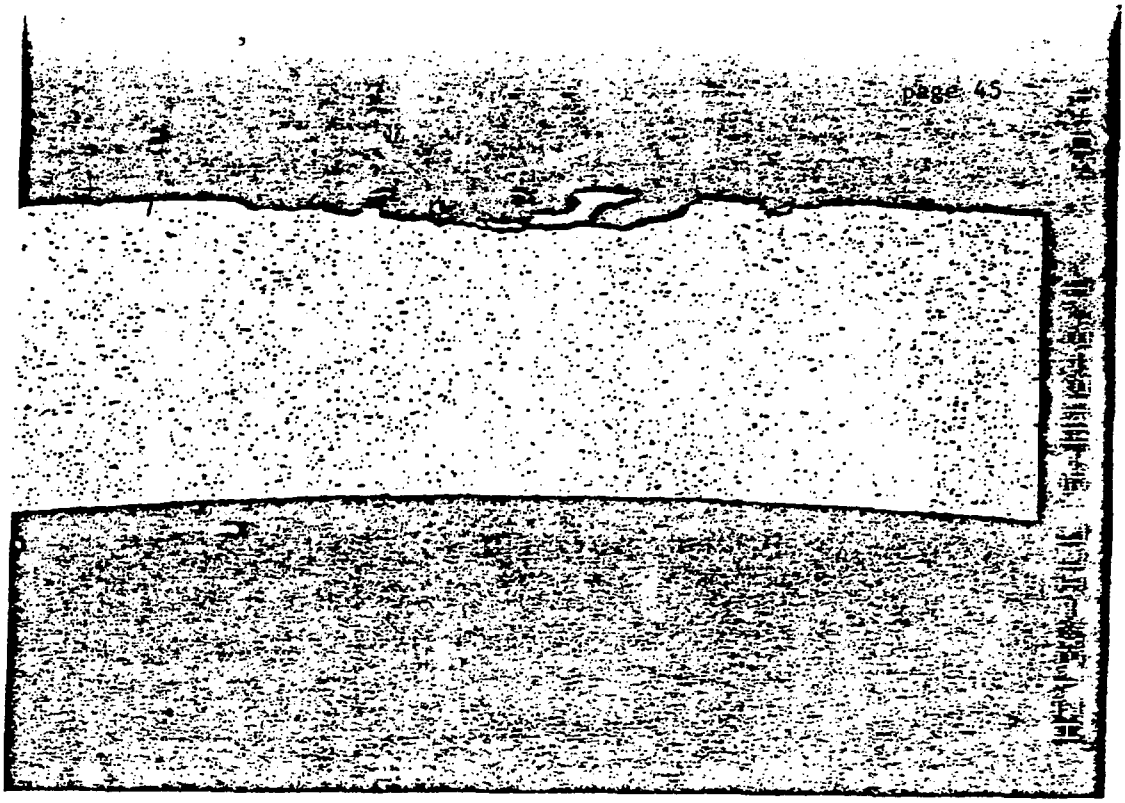

42 : Hemispherical bottom, specimen no. 2

20 : 1

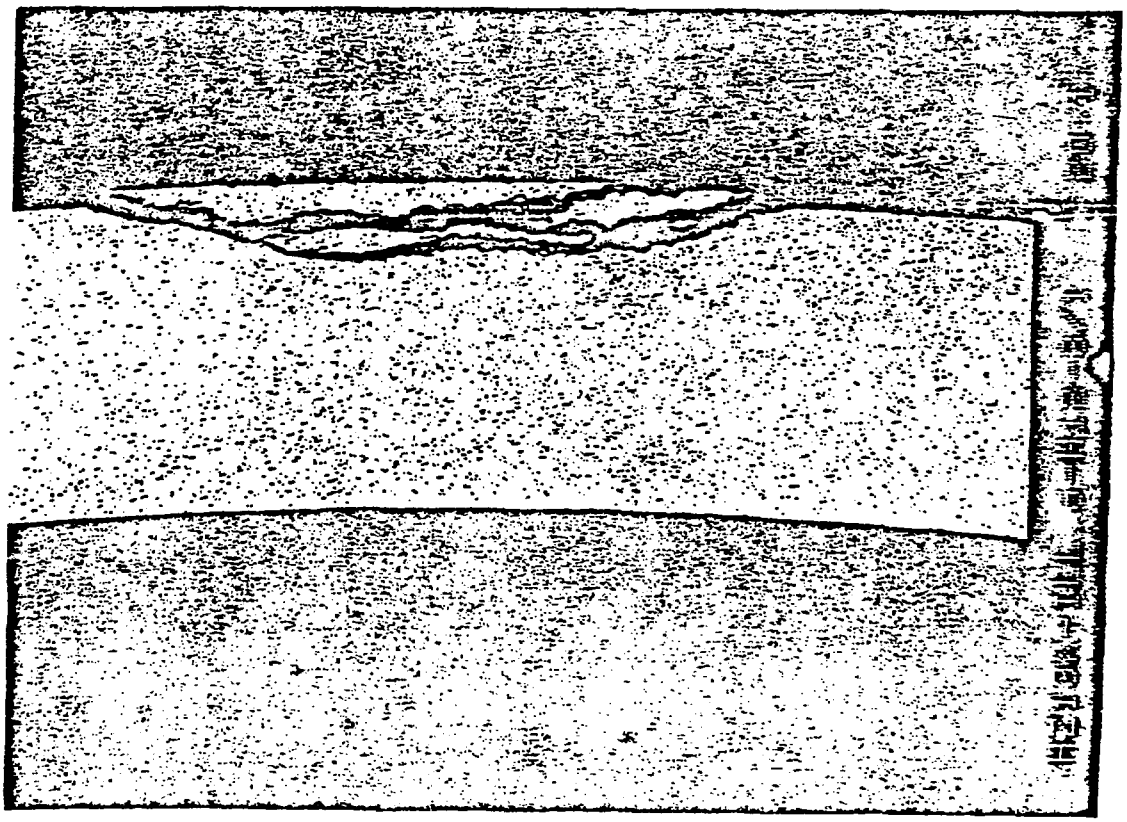

43 : Hemispherical bottom, specimen no. 3

AG3NET-RHF H12/1

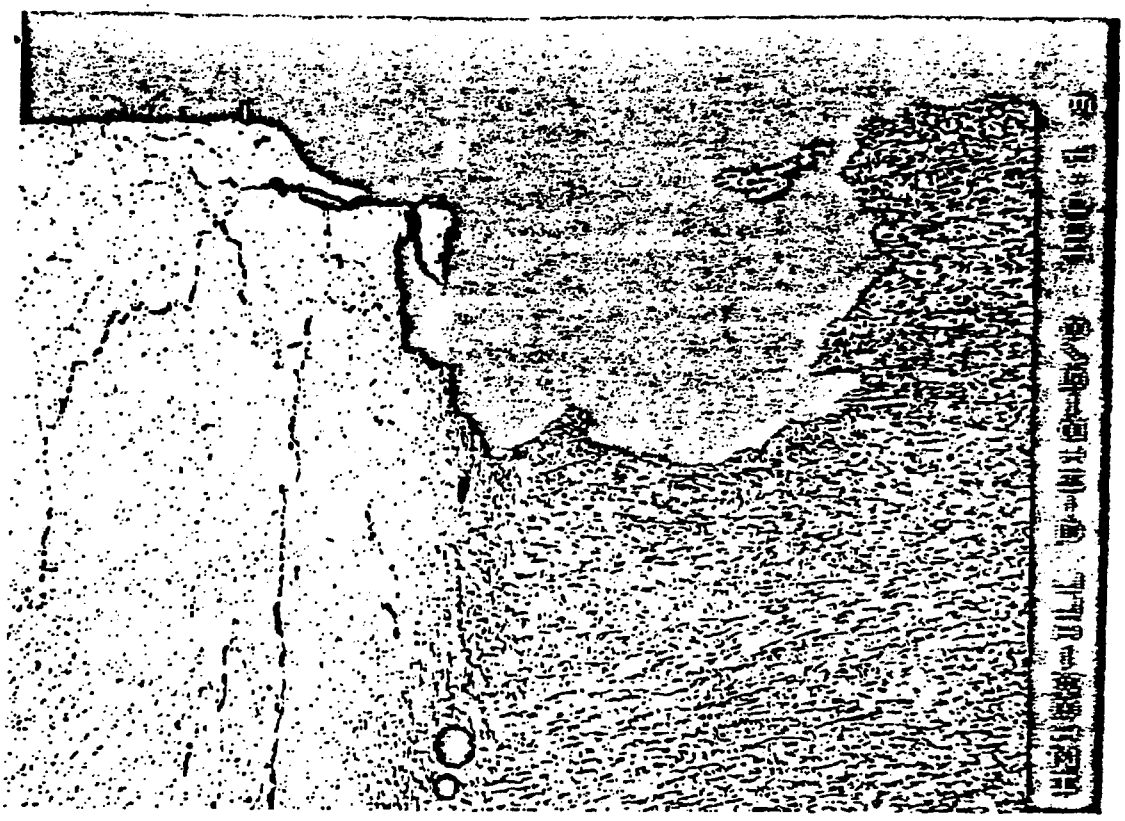

45 : Weld Bead - attacked zone
100 : 1

46 : Weld bead - crystalline structure opposite pit

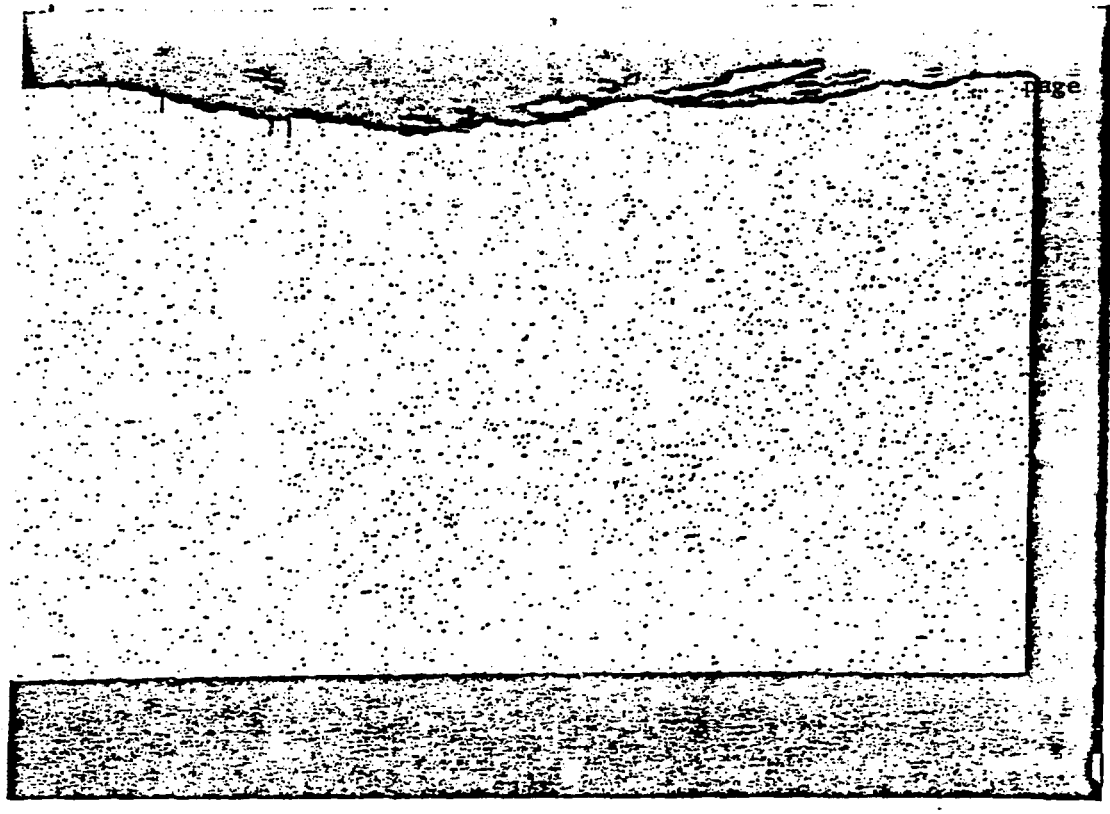

47 : Conical ferrule specimen No. 6
20 : 1

48 : Conical ferrule, specimen No. 6